

## A MINIATURE LOW FRICTION ACTIVE MAGNETIC BEARING

Chang Y. Zhang, Ronald B. Zmood

Department of Electrical Engineering

Royal Melbourne Institute of Technology

Melbourne, Australia

### ABSTRACT

In this paper we discuss the analytical analysis of the pole face design for an axial symmetric active magnetic bearing. The only condition, required for keeping the bearing stable in the passively suspended degrees of freedom (DOF's), is that the positive restoring forces and torques is able to be generated by the bearing. The pole face design is important to ensure that this condition can be satisfied. The pole face of a considered bearing is designed based on the analysis and the final design results indicate that both positive restoring forces and torques can be achieved.

### INTRODUCTION

A miniature axial symmetric active magnetic bearing (referred as magnetic bearing in this paper), specifically expected to have low friction, is being developed for use in instrumentation and for use a later date in micro machines. Some researchers have measured the dynamic friction for different magnetic suspension systems [1, 2]. But the direct measurement of static friction of magnetic bearings, which often have a very low value, has not been reported. An experimental prototype of an ultra-low friction magnetic bearing has been designed for the purpose of measuring its static friction

Based on the basic argument rather than theoretical analysis, Studer [3] and Downer [4] designed the pole faces, which spherically arcuate surfaces were centred on the geometric centre of the radial active magnetic bearings, to increase the restoring torque. In this paper the influence of the bearing parameters, such as the rotor and stator spherical pole face radii and the air-gap flux leakage coefficients, to the restoring force and

torque are analysed analytically. The analysis shows that the required restoring forces and torques can be achieved. Based on this analysis, design guidelines for axial symmetric magnetic bearing are obtained.

The cross-section of the magnetic bearing is given in Figure 1. As shown it consists of two stators, a rotor, a doughnut shaped permanent magnet on the rotor, and two control coils one on each stator. The rotor is constructed of two concentric tubes which are identified as the rotor inner and outer pole. Also the stators have a similar pole structure. The opposite surfaces of the stator and the rotor will be referred as the top and bottom pole faces. When the air-gap length between the top pole faces and the bottom pole faces is equal, the inner air-gap length is defined as  $l_{agi}$ , and the outer air-gap length is defined as  $l_{ago}$ . The curved pole faces of inner and outer pole have different spherical radii as  $R_r$  and  $R_s$ , and different geometric centre locations.

During the bearing operation, the rotor is actively suspended in the vertical direction along the bearing symmetric axis by an active vertical magnetic force. This force depends upon the current in the control coils, the current being adjusted by a control system.

The rotor is also passively suspended in four of the remaining five DOF's. The main external force acting on the rotor is gravity. If there are no other disturbing forces or torques, the rotor will be stably suspended between the stators.

### PROBLEM STATEMENT

In general if there is an external disturbing force applied to the rotor body horizontally, the rotor will move along with the direction of the disturbance and may also rotate about a horizontal axis. The linear and rotatory

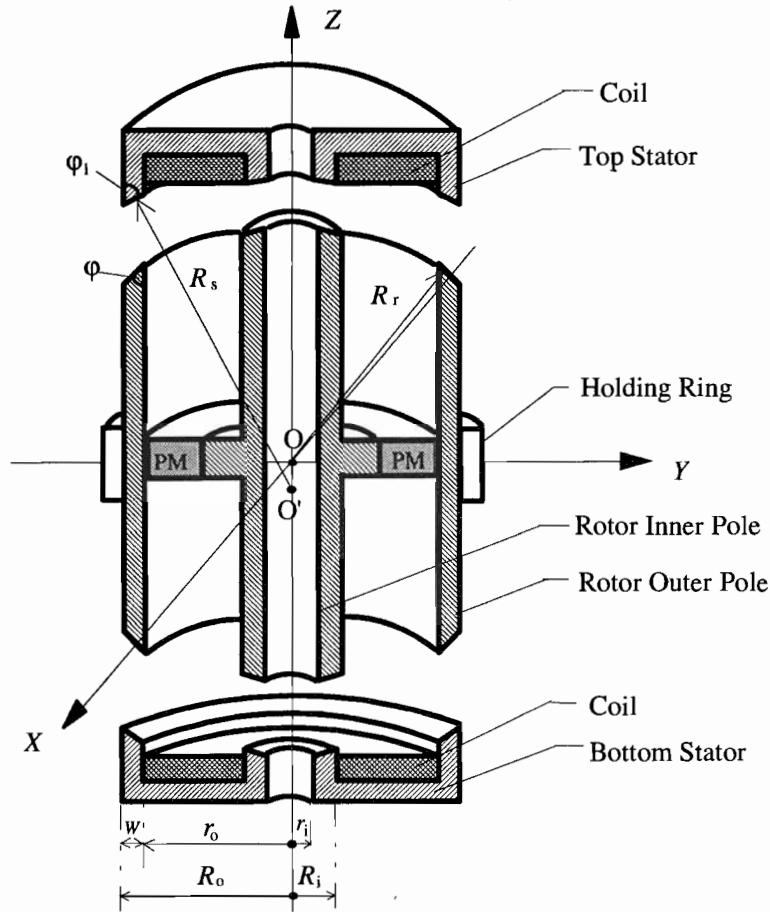


FIGURE 1: Configuration of Magnetic Bearing

movements of the rotor require that the magnetic bearing generate a restoring force and torque to stop these movements. Only if the restoring force and torque are equal or greater than the disturbance, can the rotor be suspended between the stators; otherwise the rotor will finally touch the stators.

The restoring force and torque are passively generated due to the distortion of the magnetic field between the stator and the rotor pole faces. The elementary arguments shown the restoring forces and torques only depend upon the geometric shape of the pole faces, if the flux density in the bearing air-gaps is known. For instance, if the pole faces of the stator and the rotor are spherically shaped with the same centre location, only a relatively large rotational restoring torque will be produced. If the pole faces are parallel planes, then the rotational restoring torque will be small although the translational restoring force will be relatively large.

It is assumed that both the stators and the rotor are constructed from ferromagnetic material having infinite permeability, and the magnetic motive force (MMF) across the air-gaps is constant.

### RESTORING FORCE

Firstly, the horizontal translational movement of the rotor is considered and the resultant horizontal force acting on the rotor top pole face are calculated. The simplified cross-section of the magnetic bearing is shown in Figure 2. In this figure the rotor is moved slightly to the right by a distance  $x$ . The normal forces acting to the pole faces are denoted as  $F_{ni}$  and  $F_{no}$ ; the tangential forces as  $F_{ti}$  and  $F_{to}$ . The horizontal components of the tangential forces on the inner and outer poles are referred to as  $F_{txi}$  and  $F_{txo}$  respectively. The horizontal components of the normal forces on left and right outer pole is referred as  $F_{nxi}$  and  $F_{nxr}$ . On the inner pole, the horizontal component of the tangential force almost equals to the tangential force, and the horizontal component of the normal force is approximately equal to zero. Therefore, the restoring force applied to the inner pole is dominated by the horizontal component of the tangential force.

Since the width of the cross-section of the inner and outer pole is much larger than the air-gap, and the expected maximum rotor displacement is identical to the inner air-gap length  $l_{agi}$ . The formula given by

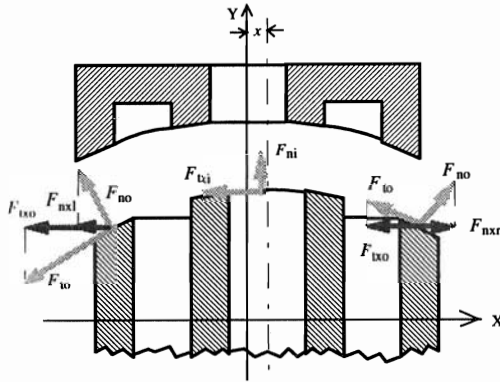


FIGURE 2: Simplified Magnetic Bearing Pole Faces

Blinn [5] and Sabins [6] can be used to find the total horizontal components of the tangential forces acting on the inner pole face.

$$F_{txi} = F_{si} \frac{4(R_i + r_i)}{\pi l_{agi}} \arcsin\left(\frac{a-1}{a+1}\right) \quad (1)$$

where:

$$F_{si} = \frac{\mu_0 \bar{g}_{agi}^2}{2} = \frac{l_{agi}^2 B_{agi}^2}{2\mu_0},$$

$$a = 1 + \frac{2x^2}{l_{agi}^2} + \sqrt{\left(1 + \frac{2x^2}{l_{agi}^2}\right)^2 - 1},$$

$B_{agi}$  is the flux density in the air-gap between the inner pole faces.

On the outer pole face:

$$F_{txo} = \frac{2(R_o + r_o)}{\pi} F_{so} \sin \varphi \arcsin\left(\frac{a-1}{a+1}\right) \times \frac{(\cot \varphi - \cot \varphi_1)W + 2l_{ago}}{\left(\frac{\cot \varphi - \cot \varphi_1}{2}W + l_{ago}\right)^2 - \left(\frac{\cot \varphi + \cot \varphi_1}{2}x\right)^2} \quad (2)$$

where:

$$F_{so} = \frac{l_{ago}^2 B_{ago}^2}{2\mu_0} = \frac{l_{ago}^2 B_{agi}^2}{2\mu_0 k^2} = \frac{l_{ago}^2 F_{si}}{l_{agi}^2 k^2}$$

$B_{ago}$  is the flux density in the air-gap between the outer pole faces

$k$  is the ratio between the flux passing through the inner pole face and the outer pole face

For constant MMF across the outer pole air-gap, the rotor, when displaced a distance  $x$  to the right, causes the flux density reduced in the left part air-gap and increased in the right part air-gap. Thus the resultant horizontal component of the normal force applied to the outer pole tends to move the rotor further to the right. The resultant horizontal component of the normal force applied to the rotor is given by

$$F_{nxo} = F_{nrx} - F_{nrx} = (2R_o - W)W l_{agi} F_{so} \cot \varphi \times (\cot \varphi + \cot \varphi_1) \left[ (\cot \varphi - \cot \varphi_1)W + 2l_{ago} \right] \left[ \frac{x}{l_{agi}} \right] \times \frac{1}{\left[ \left( \frac{\cot \varphi - \cot \varphi_1}{2}W + l_{ago} \right)^2 - \left( \frac{\cot \varphi + \cot \varphi_1}{2}x \right)^2 \right]^2} \quad (3)$$

The total restoring force  $F_r$  acting on the rotor is

$$F_r = F_{txi} + F_{txo} - F_{nxo} \quad (4)$$

### RESTORING TORQUE

If the rotor rotates clockwise about the  $x$  axis, in this paper the angle of rotation  $\beta$  is defined having the negative sign. As the rotor is rotated by a very small angle, the spherical surfaces of the rotor and stator inner poles can be considered having the same geometric centre. Using the principle of virtual work the restoring torque is found as:

$$T_i = \frac{dW_i}{d\beta} = -\frac{T_{si}}{l_{agi}} \left\{ 2 \frac{(h - R_r)(1 - \cos \beta)}{\sin \varphi_p (1 + \cos \beta)} \sqrt{\frac{R_r - h}{2h}} + 2(\pi - \varphi_p)(R_r - h) \sin \beta - [4R_r \sin \varphi_p + 4(R_r - h)(\pi - \varphi_p)] \sin \beta \right\} \quad (5)$$

where:

$$T_{si} = \frac{B_{agi}^2 l_{agi}^2 R_r}{2\mu_0}$$

$$\varphi_p = \arccos\left(-\sqrt{\frac{R_r - h}{2h}} \frac{\sin \beta}{1 + \cos \beta}\right) \quad \beta \leq 0$$

$$h = R_r - \sqrt{R_r^2 - R_i^2}$$

the restoring torque acting on the outer pole is described by

$$T_o = \frac{dW_o}{d\beta} = -2T_{so} \left\{ \frac{(h_o - h_i)R_r^2 \beta}{\sqrt{(l_{ago}^2 + (R_r \beta)^2)^3}} \times \left[ \pi + \frac{\pi(R_r \beta)^2}{4(l_{ago}^2 + (R_r \beta)^2)} - \frac{8l_{ago}(R_r \beta) \sin \varphi \sin\left(\frac{\beta}{2}\right)}{4(l_{ago}^2 + (R_r \beta)^2)} \right] + \frac{(h_o - h_i)}{\sqrt{l_{ago}^2 + (R_r \beta)^2}} \times \left[ \frac{2\pi R_r^2 \beta - 8l_{ago} R_r \sin \varphi \sin\left(\frac{\beta}{2}\right) - 4l_{ago} R_r \beta \sin \varphi \cos\left(\frac{\beta}{2}\right)}{4(l_{ago}^2 + (R_r \beta)^2)} - \frac{2R_r^2 \beta \left[ \pi(R_r \beta)^2 - 8l_{ago}(R_r \beta) \sin \varphi \sin\left(\frac{\beta}{2}\right) \right]}{4(l_{ago}^2 + (R_r \beta)^2)^2} \right] \right\} \quad (6)$$

where:

$$T_{so} = \frac{R_r l_{ago}^2 B_{ago}^2}{2\mu_0} = \frac{R_r l_{ago}^2 B_{agi}^2}{2\mu_0 k^2} = \frac{l_{ago}^2 T_{si}}{l_{agi}^2 k^2}$$

$$h_i = R_r - \sqrt{R_r^2 - r_o^2}$$

$$h_o = R_r - \sqrt{R_r^2 - r_o^2}$$

The restoring torque acting on the rotor pole is

$$T_r = T_i + T_o \tag{7}$$

**APPLICATION OF RESULTS**

The pole faces of the magnetic bearing, with the basic dimensions listed in Table 1, has been designed from the preceding analysis.

**TABLE 1:** Basic Parameters of Magnetic Bearing (Length Unit: mm)

$R_i$	$r_i$	$R_o$	$r_o$	$l_{agi}$	$l_{ago}$	$W$	$\phi$	$B_{agi}$	$R_r$	$R_s$
2.30	1.05	5.55	4.60	0.10	0.30	0.95	60.0°	0.3 T	$\frac{R_o}{\cos\phi}$	variable

Before the rotor is moved to the right or rotated clockwise the magnetic paths are axial symmetric. If the flux leakage, existing between the inner and outer pole, is ignored, the flux ratio  $k$  between the inner pole face and the outer pole face is 2.3. If the flux leakage is considered and denoted as  $k_1$ , the flux ratio, can then be expressed as  $k=2.3k_1$ .

In the following discussion, it is assumed that after the rotor has moved the flux leakage coefficient does not change. It is also assumed that the same initial values of  $B_{agi}$  and  $l_{agi}$  are used for computing the restoring forces and torques.

Taking the extreme case where the  $k_1=1$ , the rotor spherical radius  $R_r=11$  mm and the range of  $R_s$  is from 11 mm to  $\infty$ . For the rotor right translational displacement  $x$  and the negative angular displacement  $\beta$ , the restoring forces and torques are plotted in Figure 3. The positive values indicate that the magnetic bearing is able to generate a restoring force and torque in the passive DOF's and cancel the external disturbance. The negative values show that the magnetic bearing fails to prevent the rotor from further unbalanced movement in the passive DOF's. It can also be seen that under the condition  $R_r \leq R_s$ , the restoring torque is always positive but the restoring force becomes negative when the value of  $R_r$  is close to  $R_s$ . This is consistent with the basic argument. In this example  $R_s/R_r \approx 1.5$  is chosen to ensure that the both positive restoring force and torque can be achieved and both magnitudes are relatively large. The finite element analysis is used for the case of

$R_s/R_r \approx 1.5$ , where  $R_r=11$  mm and  $R_s \approx 16$  mm, and the rotor is not moved or rotated. The flux leakage coefficient between the inner and outer pole face is found to be about  $k_1 \approx 2$ . This value is twice the assumed value and mainly depending upon the air-gap length between the rotor and stator outer pole faces. The modified leakage coefficient  $k_1=2$  and the same  $R_r/R_s$  ratio (1.5) is used to recompute the restoring force and torque. The two groups of new data, together with the data for  $k_1=1$ , are plotted in Figure 4. It is apparent that the increase of the flux leakage does not seriously affect

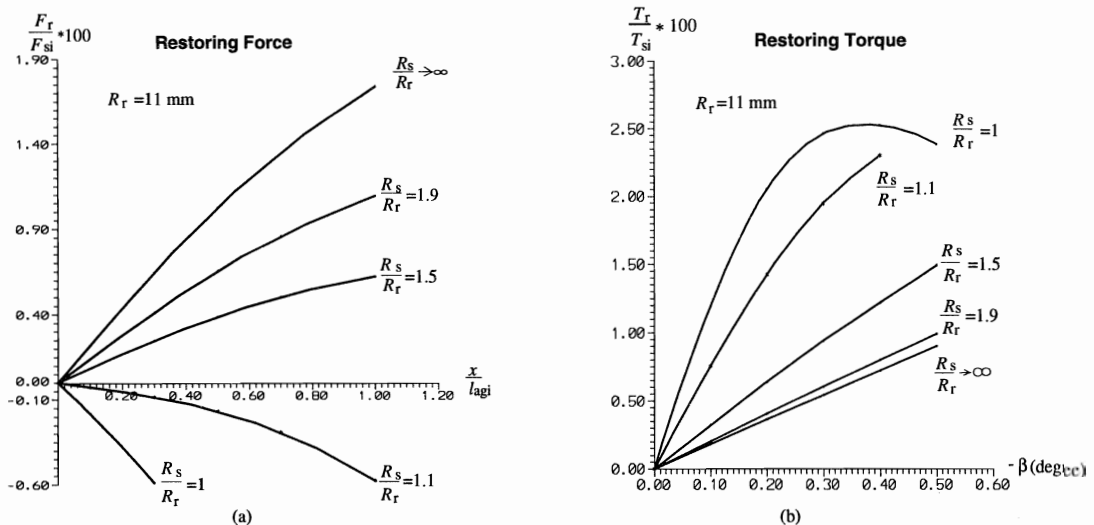


**FIGURE 3:**  $k_1=1$ , Restoring Force and Torque Curves

the restoring force, but the restoring torque is dramatically reduced. This is because the restoring force is mainly contributed by  $F_{txi}$  and this force does not depend upon the  $k_1$  so it is almost unchanged. Unlike the restoring force, the restoring torque is equally contributed by  $T_i$  and  $T_o$ . The higher the flux

From the plots it can be seen that for the same angular displacement the restoring torque keeps reducing with increasing  $k_1$ . When  $k_1=2$  and  $R_s/R_r \approx 1.2$ , the restoring torque is close to the value obtained when  $k_1=2$  and  $R_s/R_r \approx 1.5$ . This is because the leakage coefficient  $k_1$  is so high that the restoring torque is mainly decided by

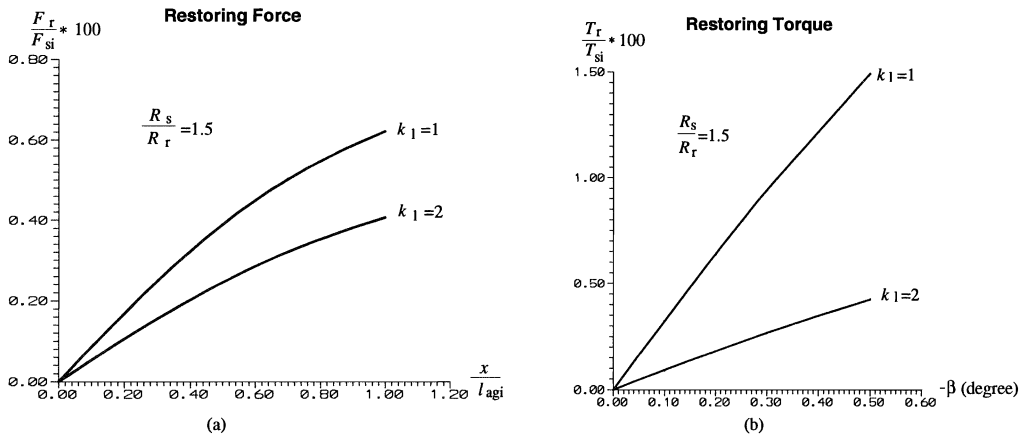


FIGURE 4:  $R_s=16$  mm,  $R_r=11$  mm, Restoring Force and Restoring Torque curves with Different Flux Leakage Coefficient

leakage coefficient is, the weaker the restoring torque acting on the outer pole will be. In the worst case the restoring torque only depends upon torque acting on the inner pole.

Several cases of  $R_s/R_r$  from 1.1 to 1.4 have been further investigated. For each case the restoring force and torque have been computed for  $k_1$  from 1.3 to 2.0. The two reasonable cases are  $R_s/R_r \approx 1.3$  and  $R_s/R_r \approx 1.2$ . Considering in the practical situation that the flux leakage will be worse than the theoretical result, the  $R_s/R_r=1.2$  is expected with a less flux leakage between the inner and outer pole. The designed value is  $R_s=13$  mm and  $R_r=11$  mm. For these values, the restoring force and restoring torque curves are plotted in Figure 5.

the torque acting on the inner pole.

From Figure 5, it is also observed that after  $R_s/R_r \leq 1.2$  the increment of the  $k_1$  causing the restoring force increase. According to the equation (4), it is found that the reduction of  $F_{nxo}$  is more sensitive to the increase of  $k_1$  than the reduction of  $F_{txo}$ .

For our magnetic bearing, the final restoring forces and torques acting on both top and bottom rotor pole faces have been computed and are listed in Tables 2 and 3.

CONCLUSION

After the translational and rotational movements of the

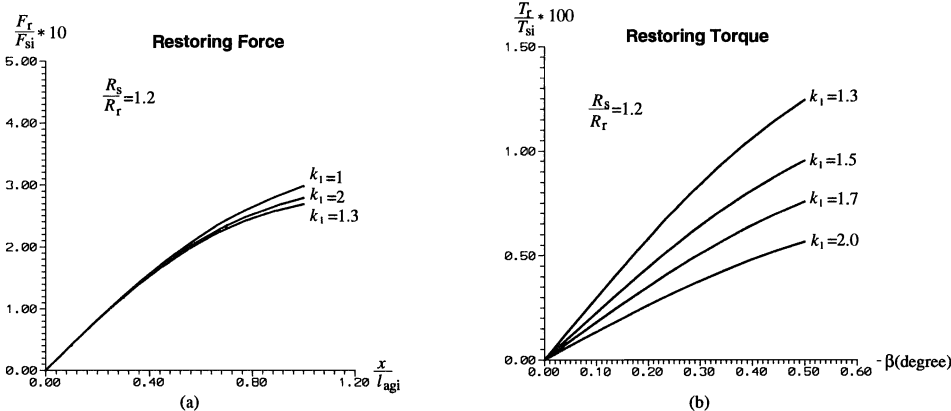


FIGURE 5:  $R_s=13$  mm,  $R_r=1.2$  mm, Restoring Force and Restoring Torque Curves with Different Flux Leakage Coefficient

TABLE 2: Radial Restoring Force  $F_r$ 

$x/l_{agi}$	0	0.1	0.3	0.5	0.7	1.0
$F_r(N)$	0	$3.4 \times 10^{-3}$	$9.8 \times 10^{-3}$	$1.5 \times 10^{-3}$	$1.9 \times 10^{-3}$	$2.2 \times 10^{-3}$

TABLE 3: Restoring Torque  $T_r$ 

$-\beta(\text{deg})$	0	0.1	0.2	0.3	0.4	0.5
$T_r(\text{Nm})$	0	$1.8 \times 10^{-4}$	$3.5 \times 10^{-4}$	$5.4 \times 10^{-4}$	$6.7 \times 10^{-4}$	$7.2 \times 10^{-4}$

rotor, the magnetic paths are no longer axial symmetric. As a consequence it is extremely difficult to compute the flux distribution in the bearing air-gaps, irrespective of whether numerical or analytical methods are used. Accurately estimating the restoring forces and torques is also considerably difficult. Nevertheless, the above analysis, which is based on a number of simplified assumptions, provides a useful approach for the preliminary design of the magnetic bearing. Although in any design there needs to be a trade-off between the magnitude of the restoring force and torque to ensure they both satisfy the required values.

## REFERENCES

1. J.K. Fremerey, "Apparatus for Determination of Residual Drag Torque on Small Spinning Spheres in Magnetic Suspension", Rev. Sci. Ins. 42(6), 1971, pp.735-762
2. W.S. Cheung, G.T. Fillies, C.H. Leyh and R.C. Ritter, "Ultra Stable Magnetic Suspensions for Rotors in Gravity Experiments", Precision Engineering, 4,1980, pp.183-186
3. P.A. Studer, "A practical Magnetic Bearing", IEEE Transaction on Magnetics Vol. MAG-13, No.5, Sept. 1977, pp.1155-1156
4. J.R. Downer, "Appendix C: Magnetic Bearing Design Analysis", NASA Contractor Report 3912, 1985, pp.87-107
5. K.J. Binns, P.J. Lawrenson, "Analysis and Computation of Electric and Magnetic Field Problems", 2nd Edition, Pergamon Press, 1973
6. A.V. Sabnis, "Analytical Techniques for Magnetic Bearings", Ph.D. Dissertation, University of California, Berkeley, 1972